

Polyisocyanides Derived from Tripeptides of Alanine

Gerald A. Metselaar, P. J. Hans M. Adams, Roeland J. M. Nolte,
Jeroen J. L. M. Cornelissen,* and Alan E. Rowan*^[a]

Abstract: Helical polymers of isocyanotripeptides derived from alanine have been synthesized and their architectures studied in detail. The helical conformation of the polyisocyanotripeptides is stabilized by internal hydrogen-bonding arrays between the tripeptide side chains. The possibility of extending the well-defined hydrogen-bonded array, from dipeptide to tripep-

ptide side chains, depends strongly on the stereochemistry of the constituent alanine amino acids, as has been shown by circular dichroism and IR studies. In polymers containing a weaker hydro-

gen-bonding array adjacent to the polymer backbone, due to steric interactions between the alanine methyl groups, a stronger second hydrogen-bonding array was present between the peptide bonds furthest away from the main chain, which is probably a result of stretching/compression of the helical-polymer conformation.

Keywords: helical structures · hydrogen bonds · polyisocyanides · stereochemistry · tripeptides

Introduction

Bulky polyisocyanides are members of a relatively small family of stable helical polymers. Other members of this family are sterically hindered poly(methacrylate ester)s,^[1] phthalocyanato-polysiloxanes,^[2] polyaldehydes,^[3] and binaphthyl-based polymers.^[4] An important condition for the stability of the helical nature of polyisocyanides is the presence of these bulky substituents, which prevent the kinetically formed helical polymer from unfolding.^[5] We have demonstrated previously that the helical backbone of a polyisocyanide can also be fixed and rigidified by incorporating pendant peptide side chains by the polymerization of suitable isocyanopeptides.^[6] The conformational stability of these polymers originates from the formation of well-defined hydrogen-bonding arrays between the peptide side chains, which run parallel to the polyisocyanide backbone. As in biomolecules, the disruption of these hydrogen-bonding arrays is a cooperative effect, as was demonstrated by ther-

mal denaturation studies in water.^[6] Intuitively, extension of the dipeptide side chains to larger peptides should lead to an even more stable helical conformation as a result of the formation of multiple hydrogen-bonding arrays along the macromolecular backbone. These more stabilized and better-defined polymers can be potentially applied as nanoscaffolds for functional groups, such as chromophores,^[7,8] redox-active groups,^[9,10] etc.,^[11] allowing them to be used in organic solar cells, as nonlinear optical materials, or as components in other nanotechnological devices. The advantages of polyisocyanotripeptides over -dipeptides for this purpose are expected to be a better thermal stability and even better-defined positioning of the functional groups with respect to each other. An onset to the investigation of isocyanotripeptides was made previously with the preparation of isocyano-L-alanyl-L-alanyl-L-alanine methyl ester and its corresponding polymer.^[6]

Herein, the nickel(II)- and acid-initiated polymerization of three different diastereomeric isocyanotripeptides based on alanine (Figure 1) and the properties of the resulting polymers are discussed, including the influence of the stereochemistry of the peptides on the reactivity of the monomers, the conformation of the polymers, and other properties. In these macromolecules, the oxygen termini of the peptides are protected as octyl esters to promote the solubility of these compounds in apolar organic solvents.

[a] Dr. G. A. Metselaar, P. J. H. M. Adams, Prof. R. J. M. Nolte,
Dr. J. J. L. M. Cornelissen, Prof. A. E. Rowan
Institute for Molecules and Materials
Radboud University Nijmegen
Toernooiveld 1, 6525 ED Nijmegen (The Netherlands)
Fax: (+31)24-365-2929
E-mail: J.Cornelissen@science.ru.nl
A.Rowan@science.ru.nl

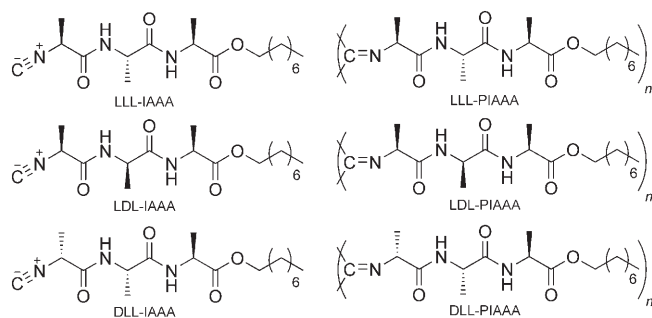
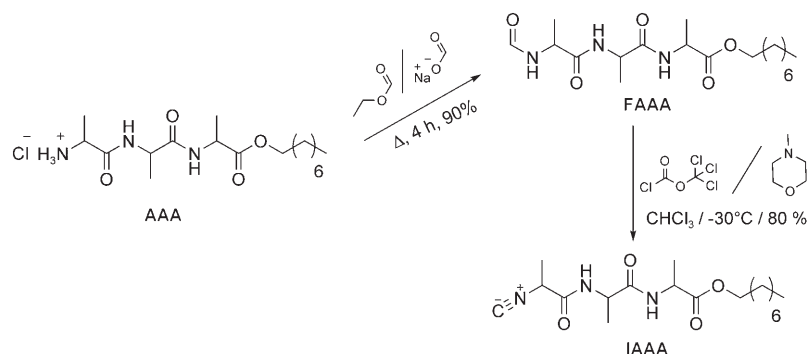


Figure 1. Alanine-based isocyanotripeptides (left) and the corresponding polyisocyanotripeptides (right).

Results and Discussion

Isocyanotrialanine octyl esters (IAAAs) were prepared from the corresponding peptides (AAAs; Scheme 1), which were synthesized by standard peptide coupling reactions. The amine as the HCl salt was reacted with ethyl formate by using sodium formate as a base to form the corresponding *N*-formyl trialanine octyl ester (FAAA). Dehydration of the formamides with diphosgene and *N*-methyl morpholine (NMM) in chloroform gave the corresponding isocyanides in 70–95% yield. All diastereomers of the isocyanotripeptides shown in Figure 1 were readily polymerized by using Ni-



Scheme 1. Synthetic route for the preparation of isocyanotripeptides.

Table 1. Selected IR and NMR spectroscopic data for the amide protons in monomers and polymers of three different diastereomers of isocyanotripeptides derived from alanine ($c = 16 \text{ mM}$ in CHCl_3).

Isocyanotripeptide		Amide A				Amide B			
		δ_{NH}	ν_{NH}	$\nu_{\text{amide I}}$	$\nu_{\text{amide II}}$	δ_{NH}	ν_{NH}	$\nu_{\text{amide I}}$	$\nu_{\text{amide II}}$
LLL-IAAA	monomer	7.02	3421	1677	1509	6.31	3421	1677	1509
	polymer	8.46	3301	1639	1549	8.10	3301	1639	1523
LDL-IAAA	monomer	7.00	3421	1677	1509	6.35	3421	1677	1509
	polymer	9.37	3264	1644	1514	6.92	3394	1677	1514
DLL-IAAA	monomer	7.00	3421	1677	1509	6.48	3421	1677	1509
	polymer	8.91	3291	1644	1525	7.41	3362	1677	1525

$(\text{ClO}_4)_2 \cdot 6\text{H}_2\text{O}$ in chloroform to yield the corresponding yellow/brown-colored polymers (PIAAAs) in $\approx 70\%$ yield.

The formation of a hydrogen-bonding network between the peptide side chains was revealed both by ^1H NMR spectroscopy, which showed a significant downfield shift for both NH protons in the trialanines upon formation of the polymers, and by IR spectroscopy, which revealed shifts in the NH stretching and the amide I and II regions (Table 1).

The chemical shifts in the ^1H NMR spectra and the wavenumbers in the IR spectra of the NH protons on going from the monomers to the polymers are dependent on the strength of the hydrogen bonds. Table 1 shows an inverse correlation between the hydrogen-bonding strength of the two different amide protons in the hydrogen-bonding array, that is, the stronger one hydrogen bond (amide A), the weaker the other one (amide B). In LLL-PIAAA, the two hydrogen bonds are almost equally strong with downfield shifts for the amide protons of $\Delta\delta = 1.4$ and 1.8 ppm, respectively. A single NH stretching vibration in the IR spectrum also shows that the two amide bonds in LLL-PIAAA are equivalent. In LDL-PIAAA (D=D-Ala), one amide shows very strong hydrogen bonding with a downfield shift of $\Delta\delta = 2.3$ ppm, whereas the other amide is only shifted downfield by $\Delta\delta = 0.6$ ppm. DLL-PIAAA appears to be an intermediate case with downfield shifts of $\Delta\delta = 1.9$ and 0.9 ppm, respectively. For these latter two diastereomeric polymers,

two distinct NH stretching frequencies were found in the IR spectra (Table 1), confirming the observations by ^1H NMR spectroscopy.

The results obtained by ^1H NMR and IR spectroscopy indicate that the chirality in the polymer formed from LLL-IAAA (L=L-Ala) allows for an equal distribution of hydrogen-bonding strength over the two amide groups present in the peptide side chains, whereas for the other two

polymers one of the two hydrogen bonds is stronger at the expense of the other. Previously, we proposed that the higher hydrogen-bonding strength of the polyisocyanodipeptide LD-PIAA with respect to its diastereomer LL-PIAA is the result of unfavorable steric interactions between the first alanine methyl group in side chain n with the second alanine methyl group in side chain $(n+1)$.^[6] These interactions also play a role in the polyisocyanotriptides, resulting in the observed differences in hydrogen-bonding strengths for the three diastereomers. These steric interactions between the alanine methyl groups, as derived from molecular mechanics force field (MMFF) calculations, are schematically depicted in Figure 2a.

The helical backbones of the polyisocyanopeptides can be considered as “polymeric springs” that can be extended or compressed depending on the hydrogen-bonding strength of the pendant peptide side chains.^[12] As a consequence, the 4_1 helical conformation, which is generally presumed to be present in the polyisocyanide architectures, is probably a 39_{10} helical conformation for polyisocyanodipeptides LL-PIAA and LD-PIAA. In related polymers containing porphyrin-functionalized alanines as side chains, an angle of 22° was found between repeat units n and $(n+4)$.^[8] An increasingly strong hydrogen-bonded amide **A** compresses the helix and simultaneously enlarges the angle between side chains n and $(n+4)$, causing the distance between amides **B** to

become too large to form stable hydrogen bonds (Figure 2b).

Chiral polyisocyanides exhibit a couplet in the CD spectra originating from the $n-\pi^*$ transitions of the imine chromophores, which is usually observed between 250 and 350 nm. For some polyisocyanodipeptides, the CD spectra display a single strong Cotton effect around $\lambda=310$ nm (Figure 3a), which has been attributed to the presence of a well-defined hydrogen-bonded network that directs all carbonyl groups in a particular array to point in the same direction. It is assumed that this ordering of amides locally creates a large permanent dipole which greatly influences the $n-\pi^*$ transitions of the imine chromophores.^[12]

The influence of the amide groups on the circular dichroic absorption of the imines enables one to study the hydrogen-bonding behavior of the polymers by using the imine chromophores as so-called “spectator groups” for the amide functions closest to the polymer backbone. Figure 3a shows a strong difference in intensity of the Cotton effect around $\lambda=310$ nm between the three different diastereomeric polyisocyanotriptides prepared at room temperature. The intense Cotton effect observed for LDL-PIAAA suggests that this polymer has a well-defined hydrogen-bonded array of amides close to the polymer backbone (amide **A** in Figure 2). To a somewhat lesser extent, the same applies for DLL-PIAAA, which shows a reversed sign for the Cotton

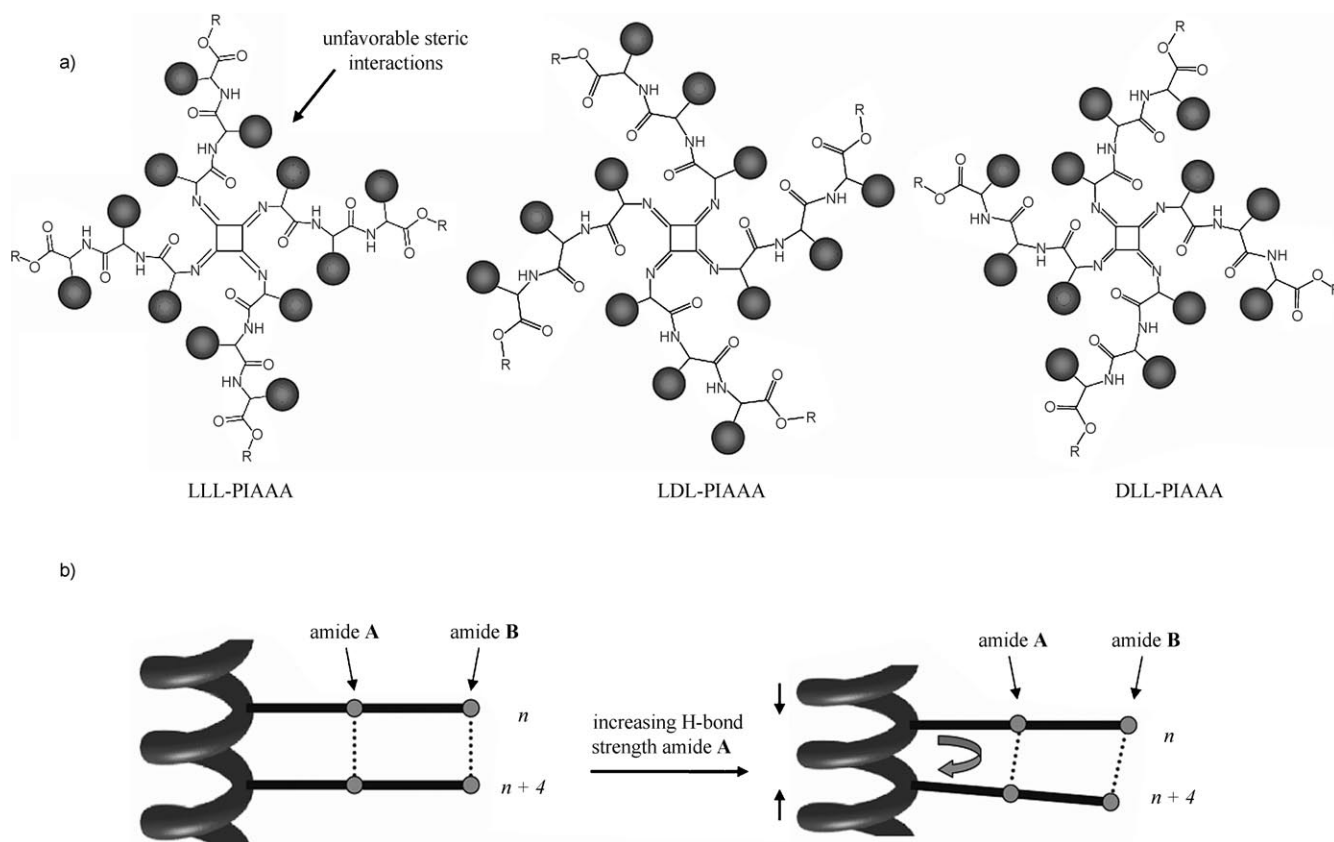


Figure 2. a) Schematic top views of the different polyisocyanotriptides showing the steric interactions between the alanine methyl groups. b) Schematic representation of the influence of hydrogen-bond strength on the distance between the amide groups in side chains n and $(n+4)$.

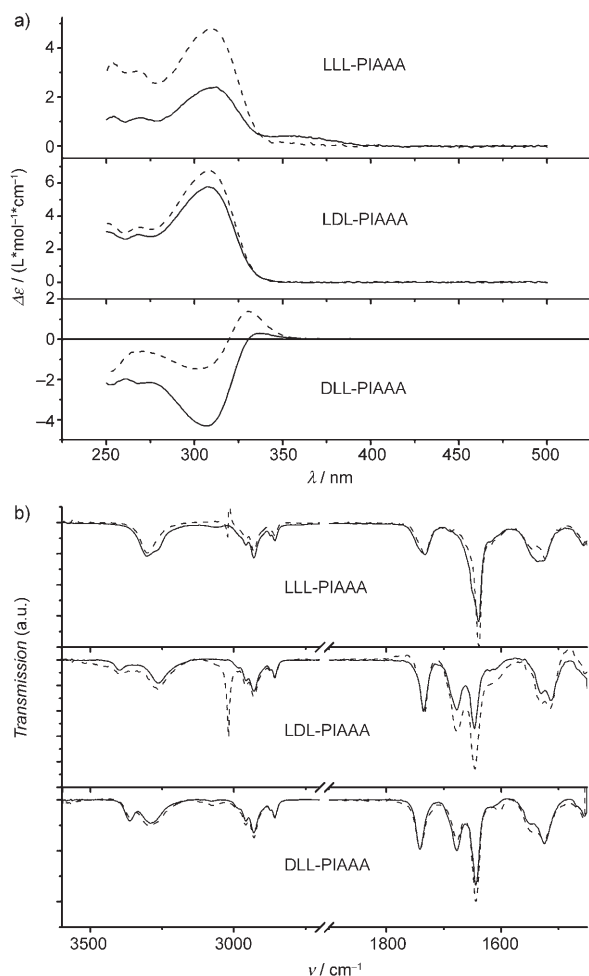


Figure 3. a) CD and b) IR spectra of polyisocyanotripeptides prepared by Ni(II) catalysis at room temperature (—) and at -30°C (----) (16 mm in CHCl_3).

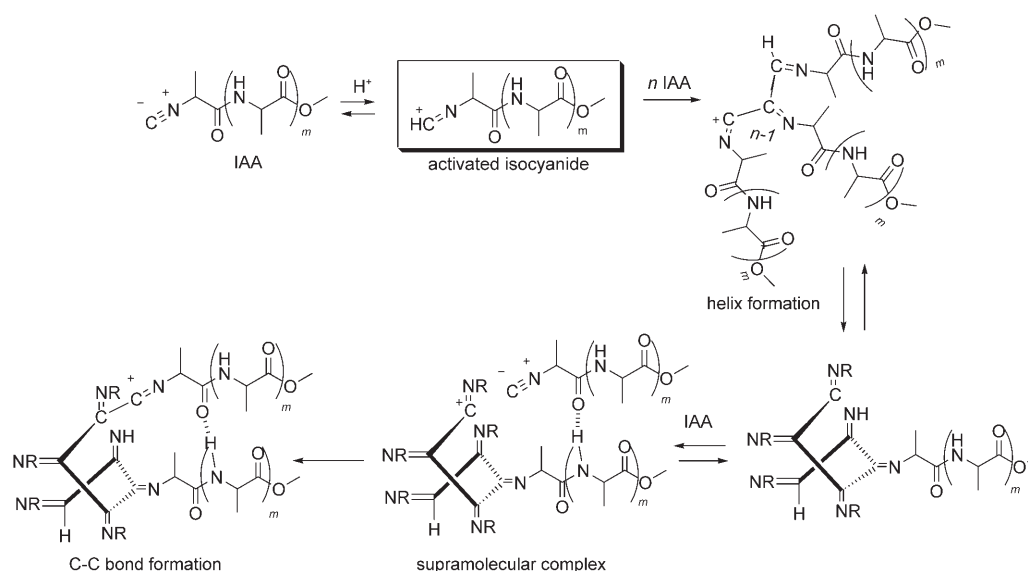
effect caused by the opposite helicity of this polymer. By far the lowest intensity of the Cotton effect is found for LLL-PIAAA, which suggests a less well-defined hydrogen-bonding array adjacent to the polyisocyanide backbone for this polymer, relative to LDL- and DLL-PIAAA.

IR and NMR spectroscopic analysis indicates that LLL-PIAAA is distinguished from the other two polymers by the presence of a hydrogen-bonded network that is well-distributed over the two different amide groups, whereas in the other two polymers only the inner amide group contributes significantly to the hydrogen-bonded conformation (vide supra). This equal distribution of hydrogen-bond strength over the two amides restricts the rotational and vibrational freedom of the side chains in LLL-PIAAA compared to the side chains in the other two polymers. As a result, defects that are incorporated in the hydrogen-bonding arrays during the fast, kinetically controlled nickel(II)-catalyzed polymerization cannot easily be corrected because of the cooperative nature of the hydrogen-bonded network between the tripeptide side chains. When the polymerization of the different IAAs was repeated at a temperature of -30°C , the CD

and IR spectra of the resulting polymers were distinctively different from those of the polymers prepared at room temperature (Figure 3). A strong increase in intensity of the Cotton effect at $\lambda=310\text{ nm}$ was observed for LLL-PIAAA when the polymerization reaction was carried out at $T=-30^{\circ}\text{C}$, which suggests a better-defined hydrogen-bonded array close to the polyisocyanide backbone. Isocyanotripeptides are capable of forming hydrogen bonds with the amide groups in other monomers or with peptide side chains in the growing polymer. It has previously been shown that the formation of a well-defined hydrogen-bonding network during polymerization significantly influences the properties of the resulting polymer.^[13] It is likely that at lower temperatures, the relatively large tripeptide chains with octyl esters form better-defined hydrogen bonds between the growing polymer chain and the monomers that are incorporated, leading to a better-defined hydrogen-bonded network.

For LDL-PIAAA, the difference between the CD and IR spectra at different temperatures was negligible, thus confirming that the second amide had little influence on the formation of a well-defined hydrogen-bonded array. Surprisingly, the intense Cotton effect seen in the CD spectrum of DLL-PIAAA prepared at room temperature was replaced by a Cotton effect that was significantly reduced in intensity when the polymerization reaction was carried out at $T=-30^{\circ}\text{C}$. The resulting CD spectrum was reminiscent of a couplet, which is usually observed for polyisocyanides that do not have a strong interaction between the $n-\pi^*$ transition of the imine chromophores and the side chains. However, despite a loss of definition in the hydrogen-bonded network close to the polymer backbone, IR spectroscopy showed that the overall hydrogen bonding between the peptide side chains in this polymer had actually increased (Figure 3b). Apparently, the conformation of the tripeptide side chains in DLL-PIAAA enables the formation of hydrogen bonds not only between amides **A** and between amides **B** in side chains n and $(n+4)$, but also “scrambling” of the hydrogen bonds between the different amides involving perhaps even esters is possible. Hence, while the influence of the amide groups in the peptide side chains on the $n-\pi^*$ transition of the imines is diminished, as was indicated by the decrease in intensity of the Cotton effect at $\lambda=310\text{ nm}$, a more elaborate but less well-defined hydrogen-bonding network is formed in DLL-PIAAA at lower temperatures.

We have previously shown that isocyanodipeptides can be polymerized by a proton-initiated process.^[14] The success of this method of polymerization proved to be very sensitive to parameters, such as temperature, solvent, acid concentration, and in particular the stereochemistry of the monomer. Based on kinetic measurements, we proposed a reaction mechanism (Scheme 2) in which initially a helical oligomer stabilized by hydrogen bonds is formed. During the propagation of the polymerization reaction, this helical prepolymer acts as a template in which the monomer is “docked” at the reactive chain end of the polymer by attractive hydrogen-bonding forces between the amide function of the monomer and the hydrogen-bonded array already present in



Scheme 2. Proposed reaction mechanism for the proton-initiated polymerization of isocyanopeptides.

the peptide side chains of the polymer. In this supramolecular complex, the thus “immobilized” monomer can readily react to form a new carbon–carbon bond, thereby extending the helical polymer.

The stereochemistry of the monomers has a dramatic effect on the reactivity in the acid-initiated polymerization.^[15] Steric interactions between the amino acid side chains can prevent the formation of stable hydrogen bonds both in the helical prepolymer and in the supramolecular complex, which leads to a drastically decreased reaction rate or even an impairment of the reaction as a whole!

Each of the three diastereomeric isocyanotripeptides was also subjected to an acid-initiated polymerization reaction. This reaction was monitored by CD and IR spectroscopy using $1/16$ equivalent of trifluoroacetic acid (TFA) as initiator. The stereochemical properties of LDL-IAAA and DLL-IAAA led to a negligible rate of polymerization under acidic conditions. For the isocyanodipeptide LD-IAA, the transition-state parameters of the acid-initiated polymerization reaction are dominated by a large unfavorable entropic factor.^[14] As a result of efficient hydrogen bonding of the monomers to the growing polymer chain, this entropic barrier can be overcome by means of a strongly favorable transition-state enthalpy. As in the isocyanotripeptides, LDL-IAAA and DLL-IAAA, only the amide closest to the polymer backbone significantly contributes to the hydrogen-bonding array, the transition-state enthalpy for these two diastereomers is approximately the same as for the isocyanodipeptide LD-IAA. The transition-state entropy, on the other hand, is significantly less favorable because of the much larger steric bulk of the additional alanine moiety and the octyl chain. This leads to the observed poor reactivity of these compounds when exposed to acid-initiated polymerization conditions. LLL-IAAA polymerized readily in the presence of acid and the shift of the NH stretching frequency from $\nu = 3422$ to 3301 cm^{-1} in the IR spectrum upon poly-

merization indicated the formation of a hydrogen-bonding network. The formation of a helical hydrogen-bonded polyisocyanide could also be concluded from the appearance of a Cotton effect at $\lambda = 308\text{ nm}$ in the CD spectrum. In the case of LLL-IAAA, the entropic penalty probably can be overcome by an enthalpic gain through the formation of a more well-defined extended hydrogen-bonded network. LLL-PIAAA formed by acid-initiated polymerization had the same conformation as LLL-PIAAA prepared by a nickel(II)-catalyzed polymerization, but had a molecular weight that was an order of magnitude higher (vide infra).

Molecular weight determination of the polyisocyanotripeptides was carried out by using atomic force microscopy (AFM; Table 2).^[15] Due to the rigid-rod character of the

Table 2. Molecular weights and polydispersity of PIAAAs prepared by nickel(II)-catalyzed polymerization at room temperature.^[a]

Polymer	M_w [kg mol ⁻¹]	M_n [kg mol ⁻¹]	$D = M_w/M_n$
LLL-PIAAA	221	188	1.2
LLL-PIAAA ^[b]	1374	731	1.9
LDL-PIAAA	183	163	1.1
DLL-PIAAA	169	133	1.3

[a] Measured by AFM. [b] Prepared by acid-initiated polymerization using $1/16$ equivalent of TFA in chloroform as the initiator.

polymers, their contour length could easily be measured. Assuming that one helical turn contains four monomers and spans a distance of $\approx 4.6\text{ \AA}$, the molecular weight as well as the dispersity of polyisocyanodipeptides prepared by both nickel(II) catalysis and acid initiation could be calculated.^[15]

The polyisocyanotripeptides formed by nickel(II) catalysis are distinctly shorter than the polyisocyanodipeptides prepared by using the same method.^[14] Their longer peptide side chain and the presence of an octyl ester instead of a methyl ester lead to more steric hindrance in the polymeri-

zation reaction. A slower propagation reaction will allow more initiation to take place, resulting in overall shorter polymers when compared to the polyisocyanodipeptides.

Like many biomolecules, the secondary structure of these polyisocyanotriptides can be disrupted by breaking up the hydrogen-bonded network through heating or treatment with acid. The irreversible effect of TFA on the secondary structure of the different diastereomeric polymers based on alanine tripeptides is shown in Figure 4, as monitored by CD and UV spectroscopy. The decrease of the intense Cotton effect at $\lambda=308$ nm for LLL-PIAAA (Figure 4a) was very rapid, and even with a 5% (v/v) TFA solution, the process was so fast that no intermediate conformations could be detected. The Cotton effect was initially replaced by weaker signals at $\lambda=353$ nm and another signal that has its maximum below $\lambda=250$ nm, which is the detection limit for CD spectroscopy when chloroform is used as the solvent. Upon standing overnight in the 5% TFA solution, the signal at $\lambda=353$ nm disappeared entirely. Simultaneously, in the UV spectrum the broad absorption band at $\lambda=353$ nm, which evolves upon addition of acid, was obscured by an absorption band that covered almost the entire visible spectrum. The appearance of absorptions at higher wavelength is a feature generally observed in the denaturation of polyisocyanopeptides, and is most probably due to a delocalization of the π electrons of the imine chromophore through an increased conjugation.

For LDL-PIAAA (Figure 4b), the change in secondary structure could be conveniently monitored by using a 10% (v/v) TFA solution. The strong Cotton effect at $\lambda=307$ nm decreased and was simultaneously replaced by a couplet with a maximum at $\lambda=360$ nm and a minimum at $\lambda=272$ nm. DLL-PIAAA proved to be very stable under acidic conditions and only started to denature at a significant rate when it was exposed to a 25% (v/v) TFA solution (Figure 4c). Also, in this case the intense Cotton effect at $\lambda=307$ nm disappeared, to be replaced by a couplet with a minimum at $\lambda=367$ nm and a maximum at $\lambda=270$ nm. In all cases, the absorption in the visible spectrum increased upon acidification, which was also visible by a brownish red coloration of the solution. This suggests the formation of a more conjugated polymer backbone when the stabilizing influence of the hydrogen-bonding network is removed.^[16]

The differences in stability under acidic conditions can be tentatively explained by the fact that in LLL-PIAAA, the peptidic side arms are firmly connected with each other at two points, which makes the polymer, going from the polymer backbone to the periphery, a relatively ordered entity with well-defined grooves at its surface (Figure 5a). These grooves enable acid to freely and easily attack the hydrogen-bonding network. LDL- and DLL-PIAAA, on the other hand, possess one strong inner hydrogen-bonding network which is probably less accessible for protons due to a more disordered and closed exterior (Figure 5b and c).

Another way to irreversibly disrupt the secondary structure of the polyisocyanotriptides is by thermal treatment. In this case, the well-defined hydrogen-bonded network is

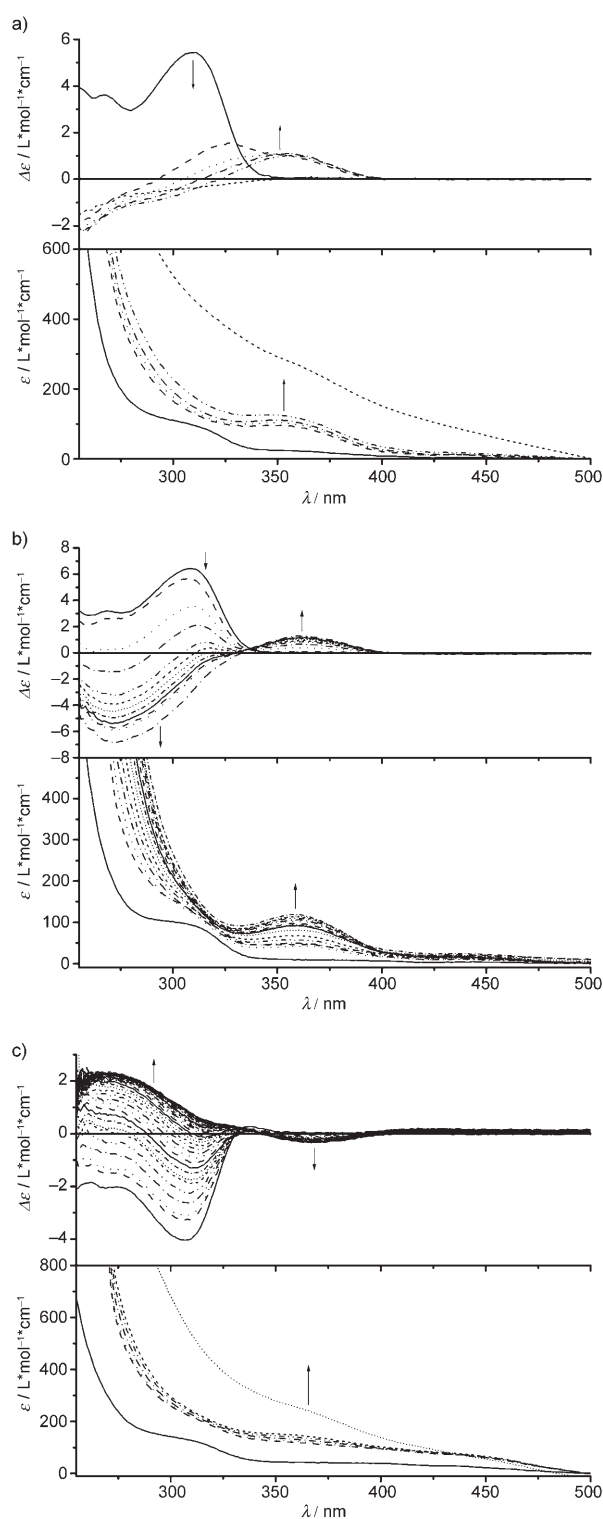


Figure 4. a) Change in the CD and UV/vis spectra upon addition of 5% (v/v) TFA to LLL-PIAAA in CHCl_3 from 0 to 30 min; (.....) is the spectrum after standing overnight. b) The same as mentioned above for LDL-PIAAA from 0 to 90 min, but with 10% (v/v) TFA in CHCl_3 ; (---) is the overnight spectrum. c) The same as mentioned above for DLL-PIAAA in CHCl_3 from 0 to 900 min (complete denaturation after ≈ 400 min), but with 25% (v/v) TFA; UV at 0, 73, 92, 115, 125, 130, and 832 min.

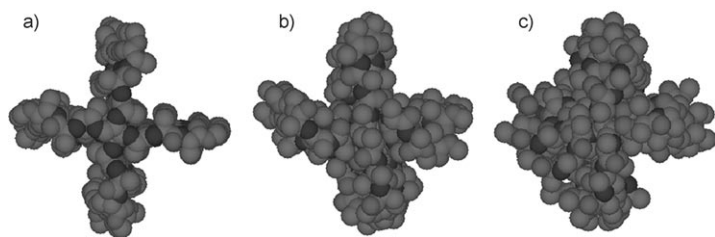


Figure 5. Top view of Corey-Pauling-Koltun (CPK) models for the three different diastereomeric polyisocyanotriptides. a) LLL-PIAAA, b) LDL-PIAAA, and c) DLL-PIAAA; the octyl tails have been omitted for clarity.

disrupted without the aid of additives, such as acid, and the accessibility of the hydrogen bonds will therefore play a less important role. Thermal stability is probably a better indication of the strength of the hydrogen-bonding network than the previously discussed stability under acidic conditions.

The polyisocyanotriptides were heated in a solution of tetrachloroethane and the disruption of the hydrogen-bonding network was again monitored by the decrease of the Cotton effect at $\lambda \approx 310$ nm (Figure 6). Figure 6a shows that at a temperature of 110°C , LLL-PIAAA undergoes a two-step disruption of the secondary structure. This process can be explained by the subsequent disruption of the inner and outer hydrogen-bonding arrays. More experiments, however, are needed to verify this proposal. Similar cooperative behavior in the thermal denaturation of the Na salt of LLL-PIAAA in water has been observed previously,^[6] and for the peptide β sheets it has been proposed that the formation and disruption of hydrogen bonds occurs cooperatively in a direction perpendicular to the strand.^[17]

In contrast, both LDL-PIAAA and DLL-PIAAA have only one strong hydrogen-bonding array between the peptide side chains, which is the one formed between the amide groups closest to the polymer backbone (amide **A**, Figure 2). Therefore, a single process is expected for the thermal disruption of the secondary structure of these polymers in line with the experiments (Figure 6b and c).

The thermal disruption of the secondary structure of LDL-PIAAA and DLL-PIAAA was found to follow first-order kinetics. The transition-state parameters for this disruption process were determined from the rate constants at different temperatures by using the Eyring equation (Table 3).

There is a remarkable difference between the transition-state parameters for thermal disruption of the secondary structure of the two diastereomeric polymers. The strongly unfavorable transition-state entropy for LDL-PIAAA can be tentatively explained by the fact that the side chains of LDL-PIAAA already have a relatively high degree of freedom in the native state. The relatively weak hydrogen bonds between the amides furthest from the polymer backbone allow the side chains to move freely. In the thermal disruption process this will irrevocably lead to a larger loss of entropy in the transition state in which the peptide side chains are rotationally more limited than in the initial state. In the

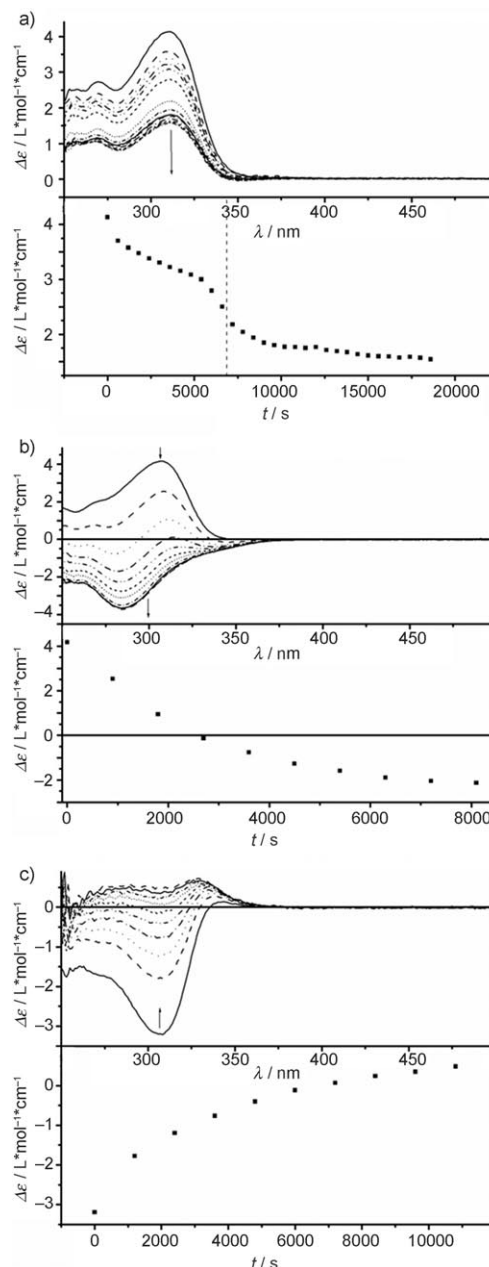


Figure 6. a) Changes in the CD spectra (top) and of $\Delta\epsilon$ at $\lambda = 308$ nm (bottom) of a solution of LLL-PIAAA (16 mM) in $\text{C}_2\text{H}_2\text{Cl}_4$. The spectra were recorded with 15 min intervals at 110°C . b) The same as mentioned above for LDL-PIAAA, with 20 min intervals at $\lambda = 307$ nm. c) The same as mentioned above for DLL-PIAAA, with 20 min intervals at $\lambda = 307$ nm.

Table 3. Transition-state parameters for the thermal disruption of LDL- and DLL-PIAAA.

Polymer	ΔH^\ddagger [kJ mol ⁻¹]	ΔS^\ddagger [J mol ⁻¹ K ⁻¹]	ΔG^\ddagger_{373} [kJ mol ⁻¹]
LDL-PIAAA	67.6	-133	117.2
DLL-PIAAA	95.4	-64	119.3

case of DLL-PIAAA, the hydrogen-bonding strength was shown to be somewhat more divided over both amide bonds of the peptide side chains (vide supra). Hence, the entropic

loss in the transition state will be less compared to that for LDL-PIAAA. The fact that ΔH^\ddagger for DLL-PIAAA is more positive than for LDL-PIAAA can be tentatively explained by the fact that in native DLL-PIAAA, the overall hydrogen-bonding strength of the amides is higher than in LDL-PIAAA, which means that a larger barrier has to be overcome in the transition state.

The rearrangement of the hydrogen bonds by thermal disruption of the secondary structure is clearly visible by IR spectroscopy (Figure 7). The IR spectra of the polymers

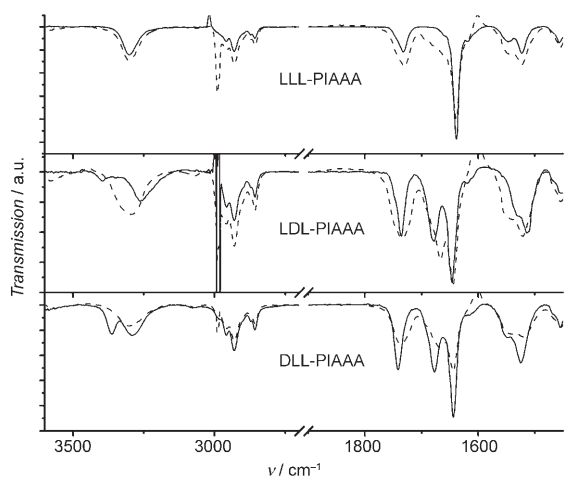


Figure 7. IR spectra in tetrachloroethane of the three different diastereomeric polyisocyanotriptides before (—) and after (----) heating at 110°C for 5 h.

after thermal treatment all showed a merging of the separate NH stretching absorptions in the “native” polymers into a broad, but single, absorption band in the denatured polymers. In addition, the separate amide I absorptions were found to shift towards each other in the denatured polymers, showing that the denaturation process can be considered as a scrambling of the hydrogen bonds to a polymer conformation in which all amide bonds contribute equally to the hydrogen-bonded network. Hence, a more elaborate but more random hydrogen-bonded network is formed upon thermal denaturation.

Conclusion

The nickel(II)-catalyzed polymerization of isocyanides derived from tripeptides of alanine results in rigid, well-defined, helical polymers that are stabilized by means of an intramolecular network of hydrogen-bonding arrays between the peptide side chains. The participation of the amide groups furthest from the polymer backbone in the formation of the hydrogen-bonding network depends strongly on the stereochemistry of the tripeptide. It is found that if the strength of the hydrogen-bonding arrays between the amide groups closest to the polymer backbone is higher, the hydrogen-bonding arrays at the periphery are less strong.

The acid-initiated polymerization of isocyanotriptides, as compared to the previously reported acid-initiated polymerization of isocyanodipeptides, is characterized by unfavorable steric interactions caused by the extension of the peptide and addition of an octyl ester. Only in the case of LLL-IAAA could the hampered reactivity, due to the increase in bulk as compared to the isocyanodipeptides, be overcome by the formation of a well-defined extended hydrogen-bonding network involving both peptide bonds of the tripeptide side chains. LLL-PIAAA formed by acid-initiated polymerization had the same conformation as the LLL-PIAAA formed by nickel(II)-catalyzed polymerization, but it had a molecular weight that was an order of magnitude higher.

Analogously to the denaturation of proteins, the secondary structure of polyisocyanotriptides could be irreversibly disrupted by treatment with strong acid or heating. The stability with respect to acid depends mostly on the accessibility of the hydrogen bonds to solvent and acid: a well-defined organization of the tripeptide side chains by extended hydrogen-bonding arrays enables protons to freely attack these hydrogen bonds, upon which the polymer is denatured. When, on the other hand, the tripeptide side chains are only bound via the inner amide bond, the disordered steric bulk of the outer amino acids and the octyl chain protect the inner hydrogen-bonding array, thereby improving the stability of these polymers under acidic conditions.

The thermal stability of the tripeptide polymers depends on the distribution of the hydrogen bonding over the two amide bonds present in each side chain. In LLL-PIAAA, both hydrogen bonds are almost equally strong and in this polymer the hydrogen-bonding network is disrupted in a cooperative manner, in which presumably first the outer and then the inner hydrogen bonds are broken. For LDL-PIAAA and DLL-PIAAA, the hydrogen-bonding strength is primarily focused on the amide bond closest to the polymer backbone. Consequently, the thermal denaturation of these polymers followed first-order kinetics. The transition-state parameters of the unfolding process could be rationalized by considering the degree of order and hydrogen bonding in the polymers prior to thermal treatment.

In summary, the formation of polyisocyanotriptides with a well-defined and stable hydrogen-bonded network is shown to depend strongly on the stereochemistry of these tripeptides, which influences the steric hindrance, helical pitch, hydrogen-bonding strength, and hence the properties of the resulting polymers.

Experimental Section

General methods and materials: Dichloromethane, chloroform, and ethyl acetate were distilled at atmospheric pressure from CaH_2 , CaCl_2 , and P_2O_5 respectively. Tetrachloroethane and *N*-methyl morpholine were distilled under reduced pressure from CaCl_2 and sodium, respectively. All other chemicals were commercial products and used as received. Flash chromatography was performed by using silica gel (0.035–0.070 mm) purchased from Acros and TLC analyses on glass coated with silica 60 F₂₅₄

from either Merck or Acros. Compounds were visualized with Cl_2 /tetramethyldiaminodiphenylmethane (TDM) or $\text{Ni}(\text{ClO}_4)_2 \cdot 6\text{H}_2\text{O}$ in EtOH. ^1H NMR spectra were recorded on Bruker WM-200 and Bruker AC-300 instruments at 297 K; ^{13}C NMR spectra were acquired on a Bruker AC-300 spectrometer. Chemical shifts are reported in ppm relative to TMS ($\delta = 0.00$ ppm) as an internal standard. FTIR spectra were recorded on Bio-Rad FTS 25 and Anadis IR300 instruments (resolution 1 cm^{-1}). CD spectra were measured on a JASCO 810 instrument. Melting points were measured on a Jeneval THMS 600 microscope equipped with a Linkam 92 temperature control unit and are reported uncorrected. EI mass spectrometry was performed on a VG 7070E instrument. Elemental analyses were determined on a Carlo Erba 1180 instrument. Optical rotations were measured on a Perkin-Elmer 241 polarimeter.

Liquid FTIR in a stirred tank reactor: FTIR measurements were carried out in a stainless steel, handcrafted, stirred tank reactor equipped with a mechanical stirrer and temperature controller. The reactor was fitted on a Bio-Rad FTS 25 instrument. In a typical experiment, the monomer (56.4 mg, 0.16 mmol) was dissolved in a solution of TFA in chloroform (1 mL, 10 mL) and added to the reactor, which was subsequently sealed from the environment. Spectra were recorded at appropriate time intervals at a stirrer speed of ≈ 200 rpm.

Atomic force microscopy: Imaging was carried out on a nanoscope III from Digital Instruments operating in the tapping mode at room temperature. Samples were prepared by spin coating (1400 rpm) a solution of polymer (1 mg L^{-1}) in chloroform on freshly cleaved mica.

Acid-induced denaturation: Solutions of polyisocyanotriptides in CHCl_3 (1.0 mg, 2.7 mL) were prepared and were transferred to a quartz cuvette with a 1.0 cm path length. A required amount of TFA was added and the unfolding processes were monitored by CD spectroscopy.

L-Alanine octyl ester hydrochloride: This compound was prepared by a literature procedure.^[18] A mixture of L-alanine (10 g, 0.11 mol), *n*-octanol (17.8 mL, 0.11 mol), and *p*-toluenesulfonate monohydrate (23.6 g, 0.12 mol) in toluene (625 mL) was refluxed until the amount of water in the Dean-Stark water trap did not increase anymore. The mixture was evaporated to dryness under reduced pressure. The residual oil was dissolved in chloroform, washed twice with 10% sodium carbonate and water, dried over MgSO_4 , and evaporated to obtain a colorless oil. Octyl L-alaninate was neutralized by a minimum amount of concentrated HCl in acetone. The solvents were evaporated in vacuo and the residual solid was recrystallized from acetone to give white crystalline L-alanine octyl ester hydrochloride (11.5 g, 52%). M.p. 115°C ; $[\alpha]_{\text{D}} = -3.2^\circ$ ($c = 1$ in CH_2Cl_2); ^1H NMR (300 MHz, CD_3CN): $\delta = 8.77$ (s, 3H; NH_3^+), 4.15 (m, 3H; $\text{OCH}_2 + \text{CH}$), 1.72 (d, $J = 7.2$ Hz, 3H; CH_3 alanine), 1.65 (m, 2H; OCH_2CH_2), 1.27 (m, 10H; CH_2), 0.88 ppm (t, $J = 6.9$ Hz, 3H; CH_2CH_3); ^{13}C NMR (75 MHz, CD_3OD): $\delta = 171.8$ (C=O), 67.5 (OCH_2), 49.9 (CH), 33.0 (CH_2), 30.3 (CH_2), 29.6 (CH_2), 26.9 (CH_2), 23.8 (CH_2), 16.4 (CH_3 alanine), 14.5 ppm (CH_2CH_3); IR (film): $\tilde{\nu} = 2950$ (CH), 1743 cm^{-1} (C=O); EIMS: m/z : 202 $[\text{M}-\text{Cl}]^+$.

L-Alanyl-L-alanyl-L-alanine octyl ester hydrochloride (LLL-AAA): This product was prepared by standard peptide coupling reactions using *tert*-butoxycarbonyl (Boc)-protected amino acids in ethyl acetate with dicyclohexylcarbodiimide (DCC) as the coupling reagent, dimethylaminopyridine (DMAP) as base, and 1-hydroxybenzotriazole hydrate (HOBT) to limit epimerization. The intermediate products were purified by extraction with 10% citric acid, NaHCO_3 , and water; these products were not characterized before use in a subsequent coupling reaction. Deprotection of the Boc-protected peptides was carried out by stirring in a HCl-saturated solution of ethyl acetate for 30 min at room temperature. The desired LLL-AAA was additionally purified by the countercurrent procedure to yield a colorless solid material (3.7 g, 77%). M.p. 174°C ; $[\alpha]_{\text{D}} = -31^\circ$ ($c = 0.50$ in CHCl_3); ^1H NMR (300 MHz, CDCl_3): $\delta = 8.44$ (s, 1H; NH), 8.10 (brs, 3H; $\text{NH}_2\text{-HCl}$), 7.79 (s, 1H; NH), 4.64 (m, 1H; CH), 4.42 (m, 2H; CH), 4.08 (m, 2H; OCH_2), 1.63 (m, 2H; OCH_2CH_2), 1.41 (d, $J = 6.9$ Hz, 6H; CH_3), 1.27 (m, 10H; CH_2), 0.88 ppm (t, $J = 6.7$ Hz, 3H; CH_2CH_3); ^{13}C NMR (75 MHz, CDCl_3): $\delta = 172.5$ (C=O), 172.0 (C=O), 171.1 (C=O), 65.7 (OCH_2), 50.0 (CH), 49.4 (CH), 48.5 (NH), 31.9 (CH_2), 29.3 (CH_2), 28.7 (CH_2), 26.0 (CH_2), 22.8 (CH_2), 18.8 (CH_3), 18.3 (CH_3), 17.9 (CH_3), 14.3 ppm (CH_2CH_3); IR: (film): $\tilde{\nu} = 3204$ (NH_3^+), 2925 (CH),

1739 (C=O), 1655 (amide I), 1548 cm^{-1} (amide II); EIMS: m/z : 344 $[\text{M}-\text{Cl}]^+$.

L-Alanyl-D-alanyl-L-alanine octyl ester hydrochloride (LDL-AAA): By using the same procedure as described for LLL-AAA, LDL-AAA was obtained in 77% yield (3.7 g) as a colorless oil. $[\alpha]_{\text{D}} = -12.2^\circ$ ($c = 0.50$ in CHCl_3); ^1H NMR (300 MHz, CDCl_3): $\delta = 9.30$ (s, 1H; NH), 9.04 (s, 1H; NH), 4.92 (m, 1H; CH), 4.49 (m, 1H; CH), 4.32 (m, 1H; CH), 4.07 (m, 2H; OCH_2), 1.60 (m, 2H; OCH_2CH_2), 1.56 (d, $J = 6.4$ Hz, 3H; CH_3), 1.45 (d, $J = 6.9$ Hz, 3H; CH_3), 1.43 (d, $J = 6.4$ Hz, 3H; CH_3), 1.28 (m, 10H; CH_2), 0.88 ppm (t, $J = 6.9$ Hz, 3H; CH_2CH_3); ^{13}C NMR (75 MHz, CDCl_3): $\delta = 175.4$ (C=O), 175.0 (C=O), 170.0 (C=O), 66.2 (OCH_2), 53.3 (CH), 50.2 (CH), 31.9 (CH_2), 29.3 (CH_2), 28.6 (CH_2), 26.0 (CH_2), 22.9 (CH_2), 18.2 (CH_3), 17.8 (CH_3), 17.3 (CH_3), 14.2 ppm (CH_2CH_3); IR: (film): $\tilde{\nu} = 3211$ (NH_3^+), 2926 (CH), 1736 (C=O), 1655 (amide I), 1548 cm^{-1} (amide II); EIMS: m/z : 343 $[\text{M}-\text{HCl}]^+$.

D-Alanyl-L-alanyl-L-alanine octyl ester hydrochloride (DLL-AAA): By using the same procedure as described for LLL-AAA, DLL-AAA was obtained in 87% yield (4.2 g) as sticky colorless crystals. $[\alpha]_{\text{D}} = 53.6^\circ$ ($c = 0.76$ in CHCl_3); ^1H NMR (300 MHz, CDCl_3): $\delta = 8.61$ (s, 1H; NH), 7.87 (s, 1H; NH), 4.64 (m, 1H; CH), 4.43 (m, 1H; CH), 4.35 (m, 1H; CH), 4.08 (m, 2H; OCH_2), 1.59 (m, 2H; OCH_2CH_2), 1.59 (d, $J = 5.9$ Hz, 3H; CH_3), 1.44 (d, $J = 6.9$ Hz, 3H; CH_3), 1.42 (d, $J = 6.3$ Hz, 3H; CH_3), 1.27 (m, 10H; CH_2), 0.88 ppm (t, $J = 6.9$ Hz, 3H; CH_2CH_3); ^{13}C NMR (75 MHz, CDCl_3): $\delta = 172.7$ (C=O), 172.5 (C=O), 170.1 (C=O), 65.6 (OCH_2), 49.4 (CH), 49.3 (CH), 48.9 (CH), 31.9 (CH_2), 29.3 (CH_2), 28.7 (CH_2), 26.0 (CH_2), 22.8 (CH_2), 18.6 (CH_3), 17.9 (CH_3), 17.5 (CH_3), 14.3 ppm (CH_2CH_3); FTIR: $\tilde{\nu} = 3202$ (NH_3^+), 2926 (CH), 1737 (C=O), 1653 (amide I), 1550 cm^{-1} (amide II); EIMS: m/z : 344 $[\text{M}-\text{Cl}]^+$.

N-Formyl-L-alanyl-L-alanyl-L-alanine octyl ester (LLL-FAAA): Sodium formate (2.96 g, 41.6 mmol) was added to a suspension of LLL-AAA (4.00 g, 10.4 mmol) in ethyl formate (250 mL) and the reaction mixture was heated to reflux for 4 h. The volatile parts were evaporated and the product was extracted from the residual yellow solid with chloroform. The resulting off-white material was recrystallized from ethanol/diisopropyl ether to give a 91% yield (3.52 g) of white crystalline LLL-FAAA. M.p. $176\text{--}177^\circ\text{C}$; $[\alpha]_{\text{D}} = -41^\circ$ ($c = 0.45$ in CHCl_3); ^1H NMR (300 MHz, CDCl_3): $\delta = 8.18$ (s, 1H; C(O)H), 7.16 (d, $J = 7.7$ Hz, 2H; NH), 7.04 (d, $J = 7.7$ Hz, 1H; NH), 4.75 (m, 1H; CH), 4.71 (m, 1H; CH), 4.55 (m, 1H; CH), 1.65 (m, 2H; OCH_2CH_2), 1.42 (d, $J = 7.2$ Hz, 3H; CH_3), 1.41 (d, $J = 6.9$ Hz, 3H; CH_3), 1.41 (d, $J = 6.9$ Hz, 3H; CH_3), 1.29 (m, 10H; CH_2), 0.88 ppm (t, $J = 6.9$ Hz, 3H; CH_2CH_3); ^{13}C NMR (75 MHz, CDCl_3): $\delta = 172.5$ (C=O), 171.3 (C=O), 171.1 (C=O), 160.4 (HC=O), 65.8 (OCH_2), 49.0 (CH), 48.4 (CH), 47.6 (CH), 31.9 (CH_2), 29.3 (CH_2), 28.7 (CH_2), 26.0 (CH_2), 22.8 (CH_2), 19.6 (CH_3), 19.3 (CH_3), 18.5 (CH_3), 14.3 ppm (CH_2CH_3); IR: $\tilde{\nu} = 3278$ (NH), 2927 (CH), 1740 (C=O), 1666, 1635 (amide I), 1547 cm^{-1} (amide II); EIMS: m/z : 372 $[\text{M}+\text{H}]^+$; elemental analysis calcd (%) for $\text{C}_{18}\text{H}_{33}\text{N}_3\text{O}_5 \cdot 1/2\text{H}_2\text{O}$: C 56.82, H 9.01, N 11.04; found: C 56.56, H 8.83, N 11.15.

N-Formyl-L-alanyl-D-alanyl-L-alanine octyl ester (LDL-FAAA): LDL-FAAA was synthesized according to the procedure described for LLL-FAAA, by using LDL-AAA (3.5 g, 9.1 mmol) as the starting compound to yield 2.70 g (80%) of white crystalline product. M.p. $132\text{--}133^\circ\text{C}$; $[\alpha]_{\text{D}} = -11.6^\circ$ ($c = 0.68$ in CHCl_3); ^1H NMR (300 MHz, CDCl_3): $\delta = 8.17$ (s, 1H; C(O)H), 7.04 (d, $J = 7.4$ Hz, 1H; NH), 6.89 (d, $J = 7.7$ Hz, 1H; NH), 6.67 (d, $J = 6.9$ Hz, 1H; NH), 4.57 (m, 3H; CH), 4.11 (m, 2H; OCH_2), 1.63 (m, 2H; OCH_2CH_2), 1.42 (d, $J = 6.1$ Hz, 3H; CH_3), 1.41 (d, $J = 7.2$ Hz, 3H; CH_3), 1.40 (d, $J = 6.9$ Hz, 3H; CH_3), 1.29 (m, 10H; CH_2), 0.88 ppm (t, $J = 6.8$ Hz, 3H; CH_2CH_3); ^{13}C NMR (75 MHz, CDCl_3): $\delta = 172.7$ (C=O), 171.4 (C=O), 171.1 (C=O), 160.8 (HC=O), 65.8 (OCH_2), 48.9 (CH), 48.3 (CH), 47.9 (CH), 31.9 (CH_2), 29.3 (CH_2), 28.7 (CH_2), 26.0 (CH_2), 22.8 (CH_2), 18.4 (CH_3), 18.3 (CH_3), 14.3 ppm (CH_2CH_3); IR: (film): $\tilde{\nu} = 3280$ (NH), 2927 (CH), 1738 (C=O), 1666, 1634 (amide I), 1549 cm^{-1} (amide II); EIMS: m/z : 372 $[\text{M}+\text{H}]^+$; elemental analysis calcd (%) for $\text{C}_{18}\text{H}_{33}\text{N}_3\text{O}_5 \cdot 1/2\text{H}_2\text{O}$: C 56.82, H 9.01, N 11.04; found: C 57.57, H 9.03, N 11.21.

N-Formyl-D-alanyl-L-alanyl-L-alanine octyl ester (DLL-FAAA): DLL-FAAA was synthesized according to the procedure described for LLL-FAAA, by using LDL-AAA (3.5 g, 9.1 mmol) as the starting compound

to yield 2.97 g (88%) of white crystalline product. M.p. 156–157°C; $[\alpha]_D^{25} = 21.6^\circ$ ($c = 0.53$ in CHCl_3); $^1\text{H NMR}$ (300 MHz, CDCl_3): $\delta = 8.18$ (s, 1H; C(O)H), 6.92 (d, $J = 7.7$ Hz, 1H; NH), 6.85 (d, $J = 7.4$ Hz, 1H; NH), 6.67 (d, $J = 7.2$ Hz, 1H; NH), 4.61 (m, 1H; CH), 4.56 (m, 2H; CH), 4.12 (m, 2H; OCH_2), 1.64 (m, 2H; OCH_2CH_2), 1.42 (d, $J = 6.9$ Hz, 3H; CH_3), 1.41 (d, $J = 7.2$ Hz, 6H; CH_3), 1.29 (m, 10H; CH_2), 0.88 ppm (t, $J = 6.8$ Hz, 3H; CH_2CH_3); $^{13}\text{C NMR}$ (75 MHz, CDCl_3): $\delta = 172.5$ (C=O), 171.2 (C=O), 171.1 (C=O), 160.7 (HC=O), 65.8 (OCH_2), 49.0 (CH), 48.4 (CH), 47.7 (CH), 31.9 (CH_2), 29.3 (CH_2), 28.7 (CH_2), 26.0 (CH_2), 22.8 (CH_2), 18.7 (CH_3), 18.6 (CH_3), 18.5 (CH_3), 14.3 ppm (CH_2CH_3); IR: (film): $\tilde{\nu} = 3280$ (NH), 2929 (CH), 1738 (C=O), 1668, 1633 (amide I), 1549 cm^{-1} (amide II); EIMS: m/z : 372 $[M+H]^+$; elemental analysis calcd (%) for $\text{C}_{18}\text{H}_{33}\text{N}_3\text{O}_5 \cdot 1/2\text{H}_2\text{O}$: C 56.82, H 9.01, N 11.04; found: C 57.62, H 8.98, N 11.15.

L-Isocyanaloalanyl-L-alanyl-L-alanine octyl ester (LLL-IAAA): *N*-Methyl morpholine (NMM; 400 μL , 3.60 mmol) was added to a solution of LLL-FAAA (0.50 g, 1.35 mmol) in chloroform (40 mL), and this solution was cooled to -30°C by using CO_2 /acetone. Diposgene (80 μL , 0.68 mmol) in chloroform (5 mL) was added dropwise over a period of 1 h, whilst maintaining the temperature at -30°C . The solution was stirred for an additional 10 min at this temperature and then brought to 0°C . Subsequently, an ice-cold solution of saturated NaHCO_3 (2 mL) was added and the reaction mixture was stirred vigorously for 5 min. The organic part was separated, extracted once with water (2 mL), and dried by using Na_2SO_4 . The solvent was evaporated and the crude light yellow product was purified by flash-column chromatography (CHCl_3 /acetone/ Et_3N 99:1:0.05 v/v/v) and subsequent recrystallization from ethanol/diisopropyl ether to yield LLL-IAAA as a white crystalline product (365 mg, 77%). M.p. 160–163°C; $[\alpha]_D^{25} = 1.5^\circ$ ($c = 0.58$ in CHCl_3); $^1\text{H NMR}$ (300 MHz, CDCl_3): $\delta = 7.02$ (d, $J = 5.9$ Hz, 1H; NH), 6.31 (d, $J = 6.9$ Hz, 1H; NH), 4.59 (m, 1H; CH), 4.44 (m, 1H; CH), 4.25 (q, $J = 7.0$ Hz, 1H; CH), 4.15 (m, 2H; OCH_2), 1.66 (d, $J = 7.1$ Hz, 3H; CH_3), 1.64 (m, 2H; OCH_2CH_2), 1.45 (d, $J = 7.2$ Hz, 3H; CH_3), 1.41 (d, $J = 7.2$ Hz, 3H; CH_3), 1.29 (m, 10H; CH_2), 0.88 ppm (t, $J = 6.8$ Hz, 3H; CH_2CH_3); $^{13}\text{C NMR}$ (75 MHz, CDCl_3): $\delta = 172.5$ (C=O), 171.2 (C=O), 171.1 (C=O), 160.7 (C \equiv N), 65.9 (OCH_2), 53.3 (CNCH), 49.3 (CH), 48.5 (CH), 31.9 (CH_2), 29.3 (CH_2), 28.7 (CH_2), 26.0 (CH_2), 22.8 (CH_2), 19.8 (CH_3), 18.7 (CH_3), 14.3 ppm (CH_2CH_3); IR: (film): $\tilde{\nu} = 3266$ (NH), 2927 (CH), 2138 (C \equiv N), 1739 (C=O), 1697, 1642 (amide I), 1553 cm^{-1} (amide II); EIMS: m/z : 353 $[M]^+$; elemental analysis calcd (%) for $\text{C}_{18}\text{H}_{31}\text{N}_3\text{O}_4$: C 61.17, H 8.84, N 11.89; found: C 61.25, H 8.93, N 11.67.

L-Isocyanaloalanyl-D-alanyl-L-alanine octyl ester (LDL-IAAA): LDL-IAAA was synthesized analogously to LLL-IAAA by starting from LDL-FAAA (500 mg, 1.35 mmol). Purification yielded LDL-IAAA as a white crystalline material (340 mg, 74%). M.p. 135°C; $[\alpha]_D^{25} = 32.6^\circ$ ($c = 0.55$ in CHCl_3); $^1\text{H NMR}$ (300 MHz, CDCl_3): $\delta = 7.00$ (d, $J = 5.4$ Hz, 1H; NH), 6.48 (d, $J = 6.4$ Hz, 1H; NH), 4.58 (m, 1H; CH), 4.48 (m, 1H; CH), 4.27 (q, $J = 7.0$ Hz, 1H; CH), 4.15 (m, 2H; OCH_2), 1.67 (d, $J = 7.2$ Hz, 3H; CH_3), 1.64 (m, 2H; OCH_2CH_2), 1.45 (d, $J = 6.4$ Hz, 3H; CH_3), 1.41 (d, $J = 6.9$ Hz, 3H; CH_3), 1.29 (m, 10H; CH_2), 0.88 ppm (t, $J = 6.8$ Hz, 3H; CH_2CH_3); $^{13}\text{C NMR}$ (75 MHz, CDCl_3): $\delta = 172.3$ (C=O), 170.2 (C=O), 165.8 (C \equiv N), 65.9 (OCH_2), 53.5 (CNCH), 49.1 (CH), 48.4 (CH), 31.9 (CH_2), 29.3 (CH_2), 28.7 (CH_2), 25.9 (CH_2), 22.8 (CH_2), 20.0 (CH_3), 18.6 (CH_3), 18.4 (CH_3), 14.3 ppm (CH_2CH_3); IR: $\tilde{\nu} = 3277$ (NH), 2929 (CH), 2143 (C \equiv N), 1732 (C=O), 1669, 1647 (amide I), 1556 cm^{-1} (amide II); EIMS: m/z : 353 $[M]^+$; elemental analysis calcd (%) for $\text{C}_{18}\text{H}_{31}\text{N}_3\text{O}_4 \cdot 1/3\text{H}_2\text{O}$: C 60.14, H 8.88, N 11.69; found: C 60.55, H 8.81, N 11.72.

D-Isocyanaloalanyl-L-alanyl-L-alanine octyl ester (DLL-IAAA): DLL-IAAA was synthesized analogously to LLL-IAAA by starting from DLL-FAAA (500 mg, 1.35 mmol), but more chloroform (90 mL) was necessary to dissolve the DLL-FAAA. Purification yielded DLL-IAAA as a white crystalline material (446 mg, 94%). M.p. 160–164°C; $[\alpha]_D^{25} = -11.3^\circ$ (CHCl_3 , $c = 0.57$); $^1\text{H NMR}$ (300 MHz, CDCl_3): $\delta = 7.02$ (d, $J = 7.2$ Hz, 1H; NH), 6.36 (d, $J = 7.2$ Hz, 1H; NH), 4.55 (m, 1H; CH), 4.44 (m, 1H; CH), 4.26 (q, $J = 7.0$ Hz, 1H; CH), 4.15 (m, 2H; OCH_2), 1.66 (d, $J = 7.2$ Hz, 3H; CH_3), 1.64 (m, 2H; OCH_2CH_2), 1.45 (d, $J = 7.2$ Hz, 3H; CH_3), 1.41 (d, $J = 7.2$ Hz, 3H; CH_3), 1.29 (m, 10H; CH_2), 0.88 ppm (t, $J = 6.8$ Hz, 3H; CH_2CH_3); $^{13}\text{C NMR}$ (75 MHz, CDCl_3): $\delta = 172.3$ (C=O),

170.2 (C=O), 165.6 (C \equiv N), 65.9 (OCH_2), 53.4 (CNCH), 49.3 (CH), 48.4 (CH), 31.9 (CH_2), 29.3 (CH_2), 28.7 (CH_2), 26.0 (CH_2), 22.8 (CH_2), 20.0 (CH_3), 18.7 (CH_3), 14.3 ppm (CH_2CH_3); IR: (film): $\tilde{\nu} = 3277$ (NH), 2930 (CH), 2145 (C \equiv N), 1737 (C=O), 1666, 1644 (amide I), 1556 cm^{-1} (amide II); EIMS: m/z : 353 $[M]^+$; elemental analysis calcd (%) for $\text{C}_{18}\text{H}_{31}\text{N}_3\text{O}_4$: C 61.17, H 8.84, N 11.89; calcd for $\text{C}_{18}\text{H}_{31}\text{N}_3\text{O}_4 \cdot 1/3\text{H}_2\text{O}$: C 60.14, H 8.88, N 11.69; found: C 60.34, H 8.78, N 11.77.

Poly(L-isocyanaloalanyl-L-alanyl-L-alanine octyl ester) (LLL-PIAAA): A solution of $\text{Ni}(\text{ClO}_4)_2 \cdot 6\text{H}_2\text{O}$ (3.66 mmol) in chloroform (2.58 mL) and a minimum amount of ethanol were added while stirring to a solution of LLL-IAAA (100 mg, 0.28 mmol) dissolved in chloroform (5 mL). After all the isocyanide had been consumed, the solvent was evaporated and the solid residue was redissolved in a minimum amount of chloroform. The LLL-PIAAA was precipitated by dropping this solution into a vigorously stirred mixture of methanol/water (3:1; 20 mL). The product was isolated by filtration and washed with methanol/water 3:1 until the filtrate remained colorless, and then once with methanol to yield LLL-PIAAA as an off-white fiberlike product (67 mg, 67%). $[\alpha]_D^{25} = -34^\circ$ ($c = 0.72$ in CHCl_3); $^1\text{H NMR}$ (300 MHz, CDCl_3): $\delta = 8.46$ (brs, 1H; NH), 8.10 (brs, 1H; NH), 5.70–3.50 (brm, 5H; CH, OCH_2), 2.00–1.00 (brm, 21H; CH_2 , CH_3), 0.87 ppm (s, 3H; CH_2CH_3); IR: (film): $\tilde{\nu} = 3284$ (NH), 2925 (CH), 1737 (C=O), 1637 (amide I), 1519 cm^{-1} (amide II); elemental analysis calcd (%) for $(\text{C}_{18}\text{H}_{31}\text{N}_3\text{O}_4)_n$: C 61.17, H 8.84, N 11.89; calcd for $(\text{C}_{18}\text{H}_{31}\text{N}_3\text{O}_4 \cdot 1/3\text{H}_2\text{O})_n$: C 60.14, H 8.88, N 11.69; found: C 60.00, H 8.64, N 11.63.

Poly(L-isocyanaloalanyl-D-alanyl-L-alanine octyl ester) (LDL-PIAAA): This compound was prepared analogously to LLL-PIAAA by starting from LDL-IAAA (100 mg, 0.28 mmol) to yield LDL-PIAAA as a light yellow solid (71 mg, 71%). $[\alpha]_D^{25} = 338^\circ$ (CHCl_3 , $c = 0.72$); $^1\text{H NMR}$ (300 MHz, CDCl_3): $\delta = 9.37$ (brs, 1H; NH), 6.92 (brs, 1H; NH), 5.30–3.70 (brm, 5H; CH, OCH_2), 2.00–1.00 (brm, 21H; CH_2 , CH_3), 0.87 ppm (s, 3H; CH_2CH_3); IR: (film): $\tilde{\nu} = 3329$ (NH), 2925 (CH), 1745 (C=O), 1676, 1645 (amide I), 1517 cm^{-1} (amide II); elemental analysis calcd (%) for $(\text{C}_{18}\text{H}_{31}\text{N}_3\text{O}_4)_n$: C 61.17, H 8.84, N 11.89; calcd for $(\text{C}_{18}\text{H}_{31}\text{N}_3\text{O}_4 \cdot 1/3\text{H}_2\text{O})_n$: C 60.14, H 8.88, N 11.69; found: C 60.62, H 8.84, N 11.61.

Poly(D-isocyanaloalanyl-L-alanyl-L-alanine octyl ester) (DLL-PIAAA): This compound was prepared analogously to LLL-PIAAA by starting from DLL-IAAA (100 mg, 0.28 mmol) to yield DLL-PIAAA as a light yellow solid (65 mg, 65%). $[\alpha]_D^{25} = -176^\circ$ ($c = 0.72$ in CHCl_3); $^1\text{H NMR}$ (300 MHz, CDCl_3): $\delta = 8.91$ (brs, 1H; NH), 7.41 (brs, 1H; NH), 5.00–3.70 (brm, 5H; CH, OCH_2), 2.00–1.00 (brm, 21H; CH_2 , CH_3), 0.87 ppm (s, 3H; CH_2CH_3); IR: (film): $\tilde{\nu} = 3358$, 3282 (NH), 2926 (CH), 1738 (C=O), 1683, 1644 (amide I), 1520 cm^{-1} (amide II); elemental analysis calcd (%) for $(\text{C}_{18}\text{H}_{31}\text{N}_3\text{O}_4)_n$: C 61.17, H 8.84, N 11.89; calcd for $(\text{C}_{18}\text{H}_{31}\text{N}_3\text{O}_4 \cdot 1/3\text{H}_2\text{O})_n$: C 60.14, H 8.88, N 11.69; found: C 60.45, H 8.76, N 11.70.

Acknowledgements

This work was supported by the Chemical Council of the Netherlands Organization for Scientific Research (NWO-CW) and the Royal Netherlands Academy for Arts and Sciences.

- [1] T. Nakano, Y. Okamoto, *Chem. Rev.* **2001**, *101*, 4013–4038.
- [2] H. Engelkamp, C. F. van Nostrum, S. J. Picken, R. J. M. Nolte, *Chem. Commun.* **1998**, 979–980.
- [3] O. Vogl, *J. Polym. Sci. Part A: Polym. Chem.* **2000**, *38*, 2293–2299.
- [4] L. Pu, *Chem. Rev.* **1998**, *98*, 2405–2494.
- [5] R. J. M. Nolte, *Chem. Soc. Rev.* **1994**, *23*, 11–19.
- [6] J. J. L. M. Cornelissen, J. J. J. M. Donners, G. A. Metselaar, R. de Gelder, W. S. Graswinckel, A. E. Rowan, N. A. J. M. Sommerdijk, R. J. M. Nolte, *Science* **2001**, *293*, 676–680.
- [7] B. Hong, M. A. Fox, *Can. J. Chem.* **1995**, *73*, 2101–2110.
- [8] P. A. J. de Witte, M. Castriciano, J. J. L. M. Cornelissen, L. Monsù-Scolaro, R. J. M. Nolte, A. E. Rowan, *Chem. Eur. J.* **2003**, *9*, 1775–1781.

- [9] D. M. Vriezema, J. Hoogboom, K. Velonia, K. Takazawa, P. C. M. Christianen, J. C. Maan, A. E. Rowan, R. J. M. Nolte, *Angew. Chem.*, **2003**, *115*, 796–800; *Angew. Chem. Int. Ed.* **2003**, *42*, 772–776.
- [10] N. Hida, F. Takei, K. Onitsuka, K. Shiga, S. Asaoka, T. Iyoda, S. Takahashi, *Angew. Chem.*, **2003**, *115*, 4485–4488; *Angew. Chem. Int. Ed.* **2003**, *42*, 4349–4352.
- [11] B. Grassi, S. Rempp, J. C. Galin, *Macromol. Chem. Phys.* **1998**, *199*, 239–246.
- [12] J. J. L. M. Cornelissen, W. S. Graswinckel, A. E. Rowan, N. A. J. M. Sommerdijk, R. J. M. Nolte, *J. Polym. Sci. Part A: Polym. Chem.* **2003**, *41*, 1725–1736.
- [13] J. J. L. M. Cornelissen, W. S. Graswinckel, P. J. H. M. Adams, G. H. Nachttegaal, A. P. M. Kentgens, N. A. J. M. Sommerdijk, R. J. M. Nolte, *J. Polym. Sci. Part A: Polym. Chem.* **2001**, *39*, 4255–4264.
- [14] G. A. Metselaar, J. J. L. M. Cornelissen, A. E. Rowan, R. J. M. Nolte, *Angew. Chem.*, **2005**, *117*, 2026–2029; *Angew. Chem. Int. Ed.* **2005**, *44*, 1990–1993.
- [15] P. Samori, C. Ecker, I. Gössl, P. A. J. de Witte, J. J. L. M. Cornelissen, G. A. Metselaar, M. B. J. Otten, A. E. Rowan, R. J. M. Nolte, J. P. Rabe, *Macromolecules* **2002**, *35*, 5290–5294.
- [16] M. Clericuzio, G. Alagona, G. Ghio, P. Salvadori, *J. Am. Chem. Soc.* **1997**, *119*, 1059–1071.
- [17] a) H. L. Schlenk, S. H. Gellman, *J. Am. Chem. Soc.* **1998**, *120*, 4869–4870; b) S. R. Griffiths-Jones, M. S. Searle, *J. Am. Chem. Soc.* **2000**, *122*, 8350–8356.
- [18] N. Yamada, K. Okuyama, T. Serizawa, M. Kawasaki, S. Oshima, *J. Chem. Soc. Perkin Trans. 2* **1996**, *12*, 2707–2714.

Received: June 29, 2006
Published online: October 18, 2006